Combined effect of hydrostatic pressure and magnetic field on the martensitic transition in the $Ni_{49}CuMn_{34}In_{16}$ alloy

M. K. Chattopadhyay,* V. K. Sharma, Anil Chouhan, Parul Arora, and S. B. Roy

Magnetic & Superconducting Materials Section, Raja Ramanna Centre for Advanced Technology, Indore 452 013, India

(Received 21 February 2011; revised manuscript received 24 June 2011; published 19 August 2011)

The combined effect of hydrostatic pressure and magnetic field on the martensitic transition in the $Ni_{49}CuMn_{34}In_{16}$ alloy is investigated through a study of electrical resistivity. It is shown that a combination of an external pressure of 2 kbar and a magnetic field of 20 kOe can produce a magnetoresistance (MR) of ∼24% in the $Ni_{49}CuMn_{34}In_{16}$ alloy at the ambient temperature of 296.5 K. The volume change in the alloy across the austenite-to-martensite phase transition is estimated to be ∼0.4%, which shows the potential of the alloy in near room-temperature actuator applications. The phase diagrams depicting the detailed field and pressure dependence of the characteristic temperatures associated with austenite-martensite phase transition are constructed from the experimental data. The results indicate that the strain fields produced in the $Ni_{49}CuMn_{34}In_{16}$ alloy are different when the alloy is cooled under externally applied pressure from what they are when the alloy is cooled in ambient pressure. These changed strain fields appear to influence the scattering of conduction electrons and the dynamics of the austenite-to-martensite phase transition in the alloy in the presence of external pressure. The present results may be useful for finding a guideline for generating chemical pressure (obtained through the partial substitution of atoms in the system) leading to newer NiMnIn alloys with room temperature functional properties.

DOI: 10.1103/PhysRevB.84.064417 PACS number(s): 75.30.Kz, 81.30.Kf

I. INTRODUCTION

The ternary off-stoichiometric Heusler alloy system $Ni_{50}Mn_{50-x}In_x$ has drawn much attention because of its interesting functional properties such as ferromagnetic shape-memory effect,[1–3] magnetic superelasticity,[4] magnetocaloric effect,[4–7] large magnetoresistance (MR),[8,9] and large magnetothermal conductivity.[10,11] The key to these functionalities is a first-order temperature and magnetic field induced martensitic transition exhibited by these alloys.[12] Recently, a very large barocaloric effect has been reported in this alloy system,[13] and it is understood that this large barocaloric effect is also a consequence of the discontinuous volume and entropy changes associated with this martensitic transition. In the $Ni_{50}Mn_{50-x}In_x$ alloys the magnetic moments are mainly confined to the Mn atoms which are magnetically coupled through Ruderman-Kittel-Kasuya-Yosida type exchange interaction.[14–16] The compositional phase diagram of the $Ni_{50}Mn_{50-x}In_x$ system of alloys was determined in detail by Sutou *et al.*,[17] where it is observed that both the austenite and martensite phases of these alloys may be either paramagnetic or ferromagnetic depending on the composition and the temperature of measurement. In many of these Heusler alloys there is a significant decrease in magnetization in the martensite phase, and this is presumably due to closer neighbor Mn–Mn positions in the martensite phase, which become antiferromagnetically coupled. The off-stoichiometric Heusler alloys such as $Ni_{50}Mn_{50-x}In_x$ contains an excess of Mn as compared to the stoichiometric compound Ni_2MnIn. The Mn–Mn distance in the off-stoichiometric alloys decreases substantially for the atomic sites where In is replaced by Mn.[18–20] These shorter bond lengths give rise to antiferromagnetic exchange interaction, which often becomes stronger in the martensite phase, though the alloys retain their overall ferromagnetic character.[4,18–21]

In a recent study on the off-stoichiometric Ni-Mn-Sn Heusler alloy system involving x-ray photoelectron spectroscopy and a first-principles density functional calculation, it was argued that in the austenite phase of this alloy system the energy of the Ni-minority spin $3de_g$ states shift towards the Fermi level due to hybridization with the $3d$ states of the antiferromagnetically coupled excess Mn atoms occupying the Sn sites.[22] It was also reported that the Jahn-Teller splitting of the Ni $3de_g$ states plays an important role in driving the martensitic transition in this alloy system.[22] In the line of these findings hybridization is expected in the $Ni_{50}Mn_{50-x}In_x$ alloys as well between the Ni $3de_g$ states and the $3d$ states of the excess Mn atoms at the In sites of the alloy. This hybridization and the Jahn-Teller splitting of the Ni $3de_g$ states are also expected to govern the magnetic properties and the magnetic and structural phase transitions in the $Ni_{50}Mn_{50-x}In_x$ system, as it does in the $Ni_{50}Mn_{50-x}Sn_x$ system. We have shown very recently that a small substitution of Ni by Cu in the $Ni_{50}Mn_{34}In_{16}$ alloy takes the martensitic transition to higher temperatures.[23] We conjectured that this stabilization of the martensite phase is achieved by the enhancement of this hybridization by the $3d^{10}$ states of Cu introduced in the system.[23] External pressure, on the other hand, is known to stabilize the martensite phase in the $Ni_{50}Mn_{34}In_{16}$ alloy by reducing the lattice parameters and the Mn–Mn distance.[24] In view of these two different routes for stabilizing the martensitic phase in the $Ni_{50}Mn_{34}In_{16}$ alloys, it is worthwhile to investigate the effect of pressure on the martensitic transition in a $Ni_{49}CuMn_{34}In_{16}$ alloy and compare the same with the parent $Ni_{50}Mn_{34}In_{16}$ alloy.[24]

In the present work we address this matter with the study of electrical resistivity of the $Ni_{49}CuMn_{34}In_{16}$ alloy as a function of temperature, pressure, and magnetic field. The $Ni_{49}CuMn_{34}In_{16}$ alloy is found to exhibit two Curie temperatures: one in the austenite phase and the other in the martensite phase. Both of the Curie temperatures are found to increase appreciably with increasing external pressure. The detailed phase diagrams depicting the effect of magnetic field and pressure on the characteristic temperatures associated with the

austenite-martensite phase transition in the $Ni_{49}CuMn_{34}In_{16}$ alloy are constructed from the experimental data. The experimental results highlight the presence of competing magnetic interactions in the alloy and the interesting role of pressure on the same. The results also show the potential of the alloy in large MR and actuator-related applications at ambient temperatures.

II. EXPERIMENTAL

A polycrystalline sample with the nominal composition of $Ni_{49}CuMn_{34}In_{16}$ was used for the present study. The actual composition of the alloy, as obtained from energy dispersive x-ray (EDX) analysis, was found to be $Ni_{48.3}Cu_{0.9}Mn_{33.9}In_{16.9}$. The details of sample preparation and characterization can be found in Ref. 23. The magnetization was measured as a function of temperature (2–390 K) using a Superconducting Quantum Interference Device Magnetometer (Quantum Design, USA). The electrical resistance was measured as a function of temperature (100–350 K) and magnetic field (up to 80 kOe) under different constant values of applied hydrostatic pressure using the AC transport option of a Physical Properties Measurement System (Quantum Design, USA). A 10 mA, 42 Hz current was used for measurements, and the temperature was varied in a strictly unidirectional manner at the rate of 0.5 K/min., both during warming up and cooling down of the sample, at all values of applied magnetic field and pressure. The sample was pressurized in a commercially available pressure cell (easyLab Technologies Ltd., UK). The hydrostatic pressure developed inside the pressure cell was estimated by measuring the resistance of a precalibrated Manganin resistor placed inside the cell along with the sample. The temperature (T) dependence of magnetization and electrical resistance at different constant values of magnetic fields (H) were measured in three different protocols, namely, zero field cooled (ZFC), field cooled cooling (FCC), and field cooled warming (FCW). In the ZFC protocol the sample is cooled down to the lowest temperature of measurement in zero field. At this temperature the magnetic field is switched on, and the measurement is performed while warming up the sample. In the FCC protocol the magnetic field is applied at a temperature much higher than the transition temperature, and the measurement is done while cooling the sample. After reaching the lowest target temperature, the measurement is continued while warming up the sample in the same magnetic field. This last protocol is called the FCW.

III. RESULTS AND DISCUSSION

Figure 1 shows the magnetization (M) versus temperature (T) plots for the $Ni_{49}CuMn_{34}In_{16}$ alloy obtained in the FCC and FCW protocols in an applied field of $H = 100$ Oe. These results have been published earlier,[23] but they are included here to make the present study self-contained. The sharp rise in magnetization while cooling down with a point of inflection at 302.2 K is attributed to the paramagnetic-to-ferromagnetic transition in the austenite phase (T_{CA}). Below 295 K the magnetization undergoes a very sharp drop and this marks the onset of the austenite-to-martensite transition in this alloy system. This latter transition is accompanied

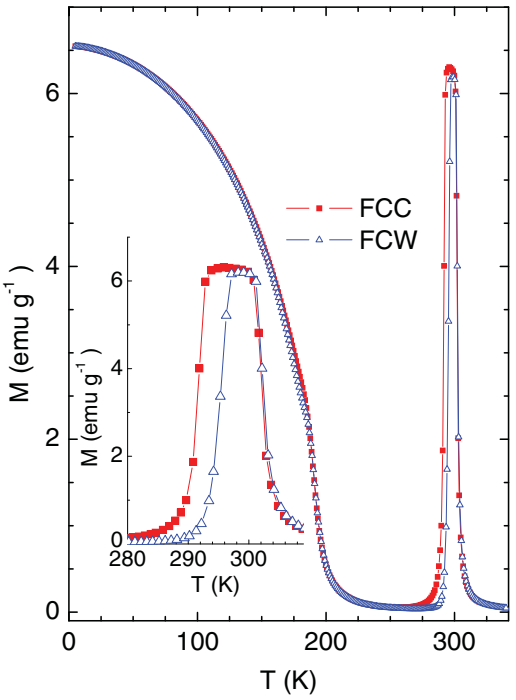

FIG. 1. (Color online) The temperature dependence of magnetization of $Ni_{49}CuMn_{34}In_{16}$ in 100 Oe magnetic field obtained using the FCC and FCW protocols. The inset shows the thermal hysteresis observed across the austenite-martensite phase transition.

by a distinct thermal hysteresis between the FCC and FCW magnetization curves highlighting the first-order nature of the phase transition (see the inset to Fig. 1). The magnetization is very low in the temperature regime just below the austenite-to-martensitic phase transition but rises again with further lowering of temperature and exhibits another point of inflection at 191.2 K. This point of inflection is attributed to a paramagnetic to ferromagnetic transition within the martensitic phase (T_{CM}).

Figure 2(a) shows the temperature dependence of electrical resistivity (ρ) of the $Ni_{49}CuMn_{34}In_{16}$ alloy in zero magnetic field under 0, 2, 4.2, and 8.1 kbar applied pressure (P). In this figure, and also in the subsequent figures, $P = 0$ actually stands for the atmospheric pressure which is 0.001 kbar. Data exist for $P = 1.3$, 3.2, and 5.6 kbar as well but are not shown here for clarity. The resistivity decreases as the temperature is decreased from 390 K (for all the values of P mentioned previously), as expected in a metallic sample. However, a change of slope is observed in the temperature dependence of resistivity below 325 K in all the curves in Fig. 2(a). This change of slope is more clearly visible on panels (b), (c), and (d) of Fig. 2 where a magnified view of the high temperature portions of some of these ρ versus T curves are shown. The ρ versus T curves for all other values of external pressure (in zero magnetic field) are not shown here for the sake of conciseness. The exact temperatures at which these changes of slopes are observed is determined from the temperature dependence of the first derivatives of these $\rho(T)$ curves. Examples of such first derivatives of the ρ versus T curves are shown on the panels (e), (f), and (g) of Fig. 2. For $P = 0$ the change of slope is observed at 302 K, which matches with the $T_{CA} = 302$ K obtained from the $M(T)$ curves. Thus this change of slope in $\rho(T)$ indicates

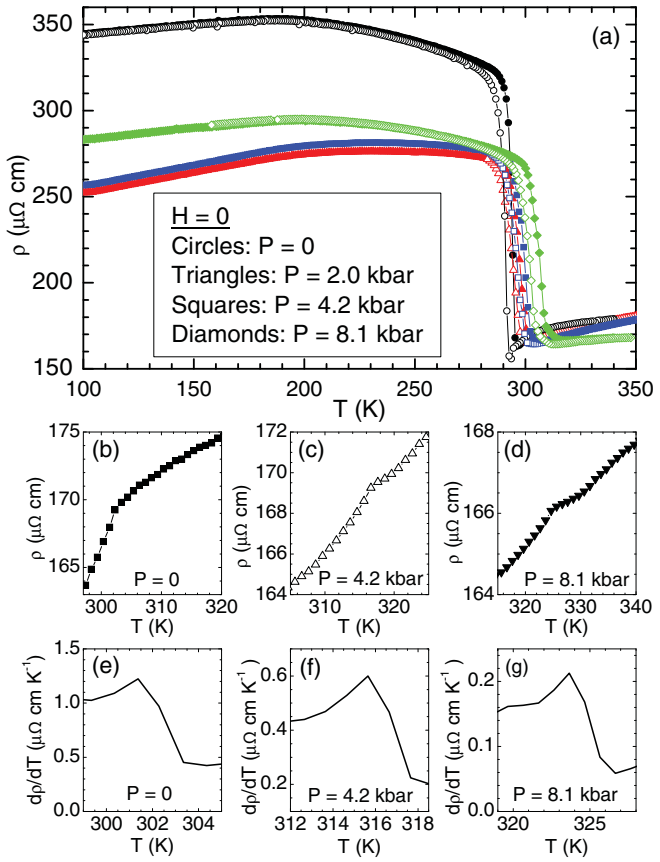

FIG. 2. (Color online) (a) The temperature dependence of electrical resistivity of the $Ni_{49}CuMn_{34}In_{16}$ alloy in zero magnetic field under different values of external pressure. Here $P = 0$ stands for zero-applied external pressure. The panels (b), (c), and (d) show the magnified view of the high temperature portions of the electrical resistivity versus temperature curves in zero magnetic field under different values of external pressure to highlight the signature of the paramagnetic to ferromagnetic transition in the austenite phase (T_{CA}) of the alloy. The panels (e), (f), and (g) show the temperature derivatives of the previous curves as functions of temperature for a clear identification of T_{CA}.

the value of T_{CA} for a particular value of P. The preciseness of the values of T_{CA} obtained from the previous ρ versus T curves for different values of P were further confirmed from the change of sign of the $d^2\rho/dT^2$ versus T curves. These curves are not presented here for the sake of conciseness. Figure 3 shows the pressure dependence of T_{CA} obtained from the $\rho(T)$ curves of Fig. 2(a). The T_{CA} is found to increase almost linearly with increasing pressure with a gradient of 2.8 K/kbar approximately. This is considerably higher than those found in the parent off-stoichiometric $Ni_{50}Mn_{34}In_{16}$ alloy (0.6 K/kbar, approximately)[24] and in the stoichiometric $Ni_{50}Mn_{25}In_{25}$ alloy (0.9 K/kbar, approximately).[25] The rate of increase of T_{CA} for the present $Ni_{49}CuMn_{34}In_{16}$ alloy is also considerably higher than the metallic ferromagnets such as Fe, Ni, and Co where the Curie temperature is found to increase at the rates of 0.10, 0.35, and 1.0 K/kbar respectively.[26] It is worthwhile to notice that though T_{CA} has been found to increase with increasing pressure in the present system of alloys and also in the Ni-Mn-Ga based off-stoichiometric Heusler alloys,[27]

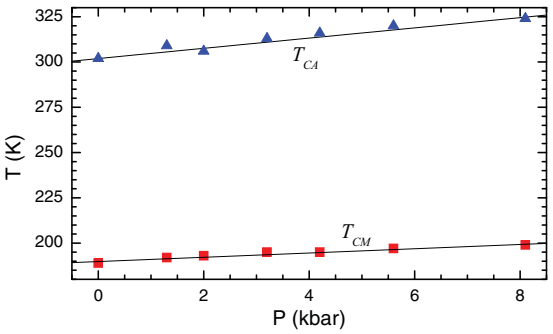

FIG. 3. (Color online) The pressure dependence of Curie temperature (determined from the change of slope observed in the temperature dependence of electrical resistivity) in the martensite and austenite phases of the $Ni_{49}CuMn_{34}In_{16}$ alloy in zero magnetic field.

it has been shown in the Ni-Mn-Sn based off-stoichiometric Heusler alloys that T_{CA} may both increase or decrease with increasing pressure depending on the actual composition of the sample.[28]

It is observed on Fig. 2(a) that the resistivity of the $Ni_{49}CuMn_{34}In_{16}$ alloy exhibits a sharp rise with decreasing temperature below T_{CA}, and this is also associated with a distinct thermal hysteresis. This sharp change in resistivity and the associated thermal hysteresis is attributed to the first order austenite-martensite phase transition in the alloy. It is observed that the resistivity is strongly affected by applied pressure in this hysteretic regime. The effect of pressure on the austenite-martensite phase transition in the $Ni_{49}CuMn_{34}In_{16}$ alloy will be discussed in more detail later in this paper, along with the effect of applied magnetic field on the same. Below this hysteretic regime, the resistivity increases with decreasing temperature and goes through a weak maximum before it starts to decrease with decreasing temperature. A similar maximum in $\rho(T)$ in the martensite phase was earlier shown to be due to the T_{CM} in a $Ni_{50}Mn_{35}In_{15}$ alloy.[29] In the present sample this maximum is observed at 189 K for $P = 0$. This matches quite well with the point of inflection observed in the low field $M(T)$ curve for the present sample in the martensite phase. Therefore, this maximum in $\rho(T)$ is taken as an indication of the value of T_{CM} for the $Ni_{49}CuMn_{34}In_{16}$ alloy for a particular value of P. Figure 3 also shows the pressure dependence of T_{CM} for the $Ni_{49}CuMn_{34}In_{16}$ alloy, apart from the pressure dependence of T_{CA}. Similar to T_{CA}, the T_{CM} is also found to increase almost linearly with increasing pressure with a large gradient of 1.2/K/kbar approximately, though this gradient is lower than that of the T_{CA} for the alloy. External pressure is expected to stabilize the martensite phase in the $Ni_{49}CuMn_{34}In_{16}$ alloy by reducing the lattice parameters and the Mn–Mn distance,[24] and thereby enhancing the antiferromagnetic exchange interaction.[4,18–22] However, the positive gradients observed in the pressure dependence of T_{CA} and T_{CM} indicate the enhancement of ferromagnetic exchange interaction both in the austenite and martensite phases.

Another significant feature observed in Fig. 2(a) is that the resistivity of the $Ni_{49}CuMn_{34}In_{16}$ alloy in the martensite phase registers a large drop in magnitude with the application of 2 kbar pressure. At higher pressures the resistivity attains

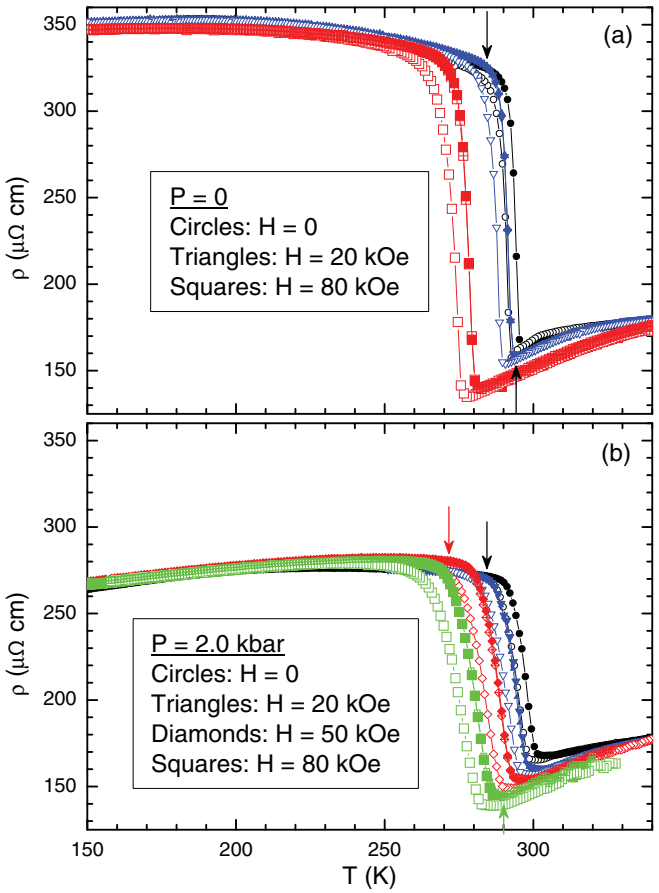

FIG. 4. (Color online) The temperature dependence of electrical resistivity in the presence of different values of magnetic field and external pressure. $P = 0$ refers to zero-applied external pressure. The open symbols represent cooling curves. The ZFC and FCW curves merge with each other. The down-arrow on panel (a) indicates the position of T_{AS} for $H = 0$. The up-arrow on the same panel indicates the position of T_{MS} for $H = 0$. The down-arrows on panel (b) indicate the positions of T_{AS} for $H = 0$ and 50 kOe. The up-arrow on panel (b) indicates the position of T_{MS} for $H = 80$ kOe. All the values of T_{AS} and T_{MS} in different values of field and pressure are not indicated on the figure for the sake of clarity. The details of the technique used for the determination of T_{AS} and T_{MS} are given in the text.

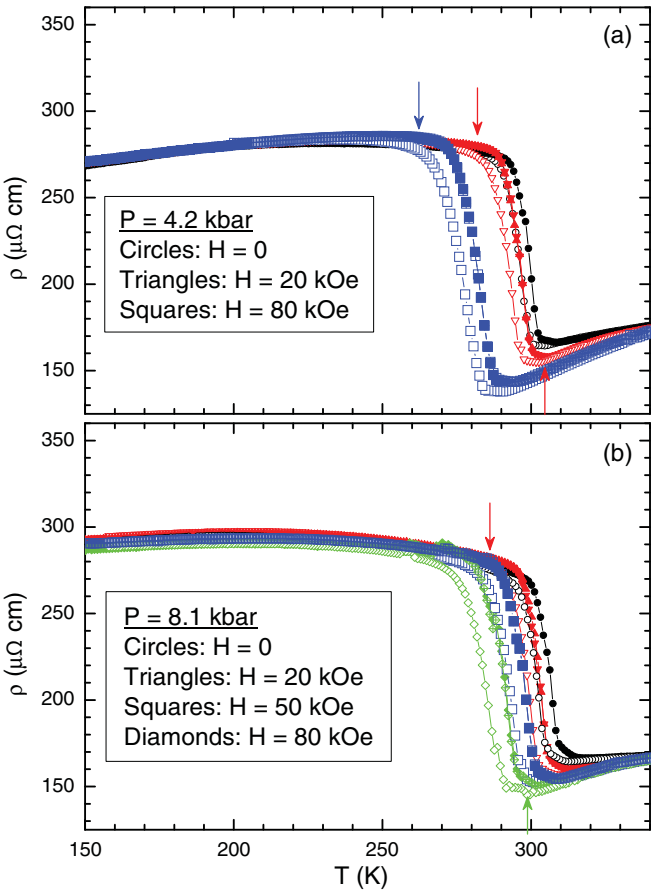

FIG. 5. (Color online) The temperature dependence of electrical resistivity in the presence of different values of magnetic field and external pressure. The open symbols represent cooling curves. The ZFC and FCW curves merge with each other. The down-arrows on panel (a) indicate the positions of T_{AS} for $H = 20$ and 80 kOe. The up-arrow on panel (a) indicates the position of T_{MS} for $H = 20$ kOe. The down-arrow on panel (b) indicates the position of T_{AS} for $H = 20$ kOe. The up-arrow on panel (b) indicates the position of T_{MS} for $H = 80$ kOe. All the values of T_{AS} and T_{MS} in different values of field and pressure are not indicated on the figure for the sake of clarity.

higher magnitudes in the martensite phase but does not attain the magnitude obtained in zero pressure. In the austenite phase, on the other hand, both the magnitude of resistivity and the overall slope of the $\rho(T)$ curves decrease with increasing pressure. Thus the magnitude of electrical resistivity of the $Ni_{49}CuMn_{34}In_{16}$ alloy shows some anomalous behavior in the martensite phase in the presence of pressure. It will be seen in the Figs. 4 and 5 (see subsequent discussion) that this anomalous behavior is not affected by applied magnetic field (up to 80 kOe) to any appreciable extent, and therefore, is not related to the magnetic interactions in the alloy. A scrutiny of Fig. 2(a) reveals that the slope of the $\rho(T)$ curve in the martensite phase of the $Ni_{49}CuMn_{34}In_{16}$ alloy under an external pressure of 8.1 kbar is different from that obtained under 2 and 4.2 kbar external pressure. In fact the difference between the curve for $P = 8.1$ kbar and the curves for $P = 2$ and 4.2 kbar is larger at 100 K than at 280 K (just below the austenite-to-martensite transition). It may be recalled that strain produced in the $Ni_{49}CuMn_{34}In_{16}$ alloy changes from about $+0.08$ to -0.02% across the austenite-to-martensite transition and from about -0.04 to -0.28% as the sample is cooled down from 280 K to 100 K (see Fig. 5 of Ref. 23). Thus a large strain is produced in the $Ni_{49}CuMn_{34}In_{16}$ alloy at the onset of the martensitic transition, which continues to build significantly well inside the martensite phase (while cooling). We conjecture that this strain is affected strongly by external pressure. The existence of strain-disorder coupling[30] is expected in the Ni-Mn-In based off-stoichiometric Heusler alloy system across the martensitic transition. This means that there is strong strain-mediated correlation between different regions of the alloy across the martensitic transition, which probably influences the nucleation and growth of phases. In our argument when the $Ni_{49}CuMn_{34}In_{16}$ alloy is cooled down inside the pressure cell after the application of the hydrostatic pressure, the strain fields produced in the alloy during the martensitic transition are different from what are obtained in

ambient pressure. This probably affects the extent of scattering of conduction electrons by the strain fields, and as a result the electrical resistivity in the martensite phase is strongly affected by the application of pressure. Moreover, the extent or nature of strain-disorder coupling may be different in the presence of pressure because of the changed strain fields, and this is likely to affect the nucleation and growth mechanism across the transition.

Figures 4 and 5 show the combined effect of pressure and magnetic field on the $Ni_{49}CuMn_{34}In_{16}$ alloy. For all the values of applied external pressure, the ZFC curves for the $Ni_{49}CuMn_{34}In_{16}$ alloy merge with the FCW curves for applied magnetic fields up to 80 kOe (within the limits of the experimental uncertainty). Comparing Figs. 2, 4, and 5, it can be seen that while pressure tends to elevate the martensitic transition in the $Ni_{49}CuMn_{34}In_{16}$ alloy towards room temperature, the magnetic field tends to shift it to the lower temperature side. All the panels of Figs. 4 and 5 are plotted on the same scale of temperature and resistivity for a clear comparison among themselves. To understand the details of the combined effect of magnetic field and pressure on the martensitic transition in the $Ni_{49}CuMn_{34}In_{16}$ alloy in terms of the standard Landau phenomenology of the first-order phase transition,[31] the field and pressure dependence of the temperatures characteristic to this transition were determined. In this phenomenological theory the free energy of a system across a phase transition may be expressed as a power series in terms of the order parameter. At the thermodynamic critical temperature for the first-order phase transition one observes the coexistence of two phases, corresponding to two minima in the free energy at two different values of the order parameter which are separated by an energy barrier. The free energy becomes asymmetric, and the energy barrier decreases as the system is cooled down or warmed up across this temperature giving rise to metastability of phases against the thermal energies present in the system. The temperature at which the energy barrier and the secondary minimum vanish defines the limit of metastability (superheating and supercooling). The hysteresis across a first-order phase transition is due to this metastability, and therefore it disappears beyond the limits of metastability.[31] The limits of metastabiliy for the first-order austenite-martensite phase transition in the $Ni_{49}CuMn_{34}In_{16}$ alloy were determined from the end points of the thermal hysteresis observed in the $\rho(T)$ curves. These are the temperatures at which the $\rho(T)$ curves corresponding to the warming up and cooling down of the sample start to overlap over one another on both sides of the austenite-martensite phase transition in the $Ni_{49}CuMn_{34}In_{16}$ alloy. These are represented by T^{**} (the limit of superheating of the martensite phase or the austenite finish temperature T_{AF}) and T^{*} (the limit of supercooling of the austenite phase or the martensite finish temperature T_{MF}), respectively.[31] However it is to be noted that these characteristic temperatures will depend on the temperature sweep rate. In the present study the same temperature sweep rate (0.5 K/min.) was maintained for doing the experiments in all values of applied magnetic field and pressure. Accordingly, these temperature limits correspond to this particular rate of temperature change. The onset of the austenite-to-martensite phase transition while cooling, T_{MS}, and the onset of martensite-to-austenite phase transition while warming, T_{AS}, were ascertained, respectively, from the onsets

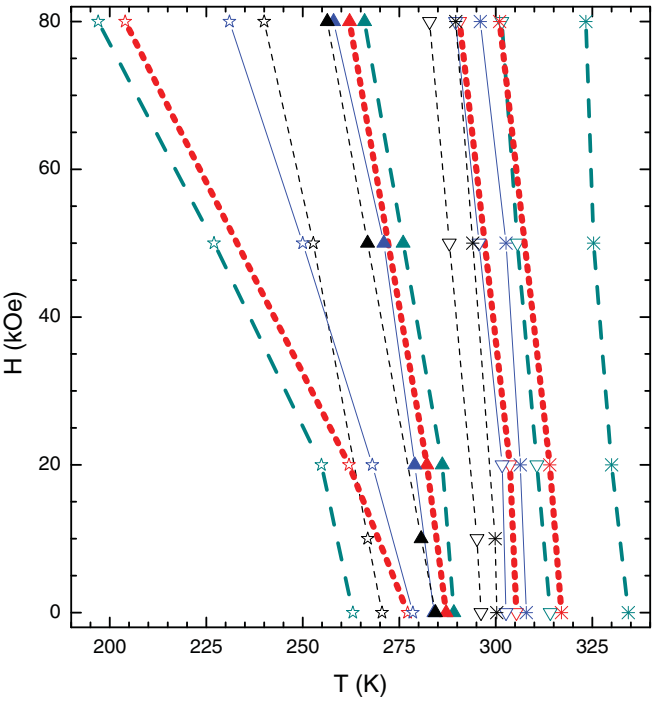

FIG. 6. (Color online) The field versus temperature-phase diagram of the $Ni_{49}CuMn_{34}In_{16}$ alloy under different values of external pressure. The open stars represent the limit of supercooling (T^{*}) of the austenite phase. The asterisks stand for the limit of superheating (T^{**}) of the martensite phase. The onset of the austenite-to-martensite phase transition while cooling down (T_{MS}) and the onset of martensite-to-austenite phase transition while warming up (T_{AS}) are represented, respectively, by open down-triangles and filled up-triangles. The fine dashed lines denote ambient pressure. The solid lines stand for 2 kbar applied external pressure. The thick dotted lines and the firm dashed lines represent 4.2 and 8.1 kbar applied external pressure, respectively.

of the sharp rise (while cooling down) and sharp fall (while warming up) observed on the $\rho(T)$ curves. The first and second derivatives of the ρ versus T curves were used to find these onsets. It is observed that the austenite-martensite transition takes place over a finite width of temperature, which indicates to the disorder influenced nature of this transition.[32] That the onset of nucleation while warming is lower than the same while cooling indicates that due to the influence of quenched disorder in the alloy, there is a landscape of the onsets of the transition[33] in the alloy. Figure 6 shows the field dependence of T^{*}, T^{**}, T_{MS}, and T_{AS} for different values of applied external pressure (see the figure caption for details). The width of the hysteresis (defined by the temperature difference between T^{*} and T^{**}) seems to increase with increasing external pressure, and the effect is more pronounced in the presence of higher magnetic fields. The T^{**}, T_{MS}, and T_{AS} lines shift toward higher temperature with increasing pressure. The T^{*} line, on the other hand, shows a different trend as a function of pressure. The variation of these characteristic temperatures as a function of external pressure is described subsequently.

Figure 7 shows the pressure dependence of T^{*}, T^{**}, T_{MS}, and T_{AS} for different constant values of applied magnetic field. It is observed that T^{**}, T_{MS}, and T_{AS} increase

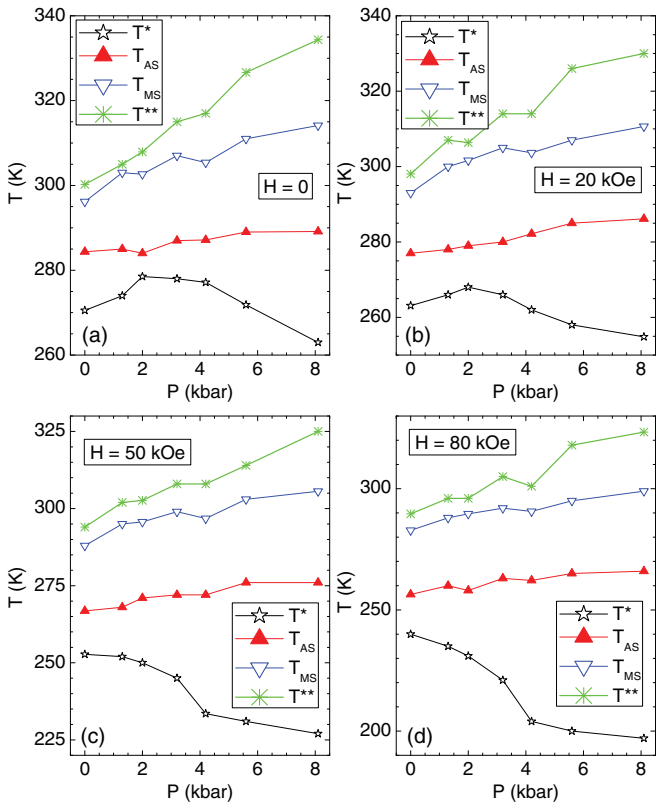

FIG. 7. (Color online) Pressure dependence of the onset temperatures and the limits of metastabilities of the $Ni_{49}CuMn_{34}In_{16}$ alloy for different applied magnetic fields.

approximately linearly with increasing pressure. The temperature T_{MS} is found to increase approximately at the rate of 2 K/kbar for all applied field values up to 80 kOe. The temperature T_{AS}, on the other hand, increases approximately at the rate of 0.7 K/kbar in zero field; however, this rate increases to 1.2 K/kbar in 80 kOe magnetic field. The limit of superheating T^{**} is found to increase at the rate of 4 to 4.2 K/kbar for all values of applied magnetic field. These values are of the same order as those reported for the parent $Ni_{50}Mn_{34}In_{16}$ alloy.[13,24] The combined effect of pressure and magnetic field on T^{*}, however, is found to be quite interesting in the $Ni_{49}CuMn_{34}In_{16}$ alloy. In zero magnetic field T^{*} initially increases with increasing external pressure, exhibits a humplike feature close to $P = 2$ kbar, and then decreases again as the pressure is increased above 4 kbar. As the magnetic field is raised to 20 kOe, this hump becomes much smaller but still continues to exist. In higher fields (50 and 80 kOe), the hump is replaced by a small steplike feature, and T^{*} decreases unidirectionally with increasing external pressure. This latter behavior of T^{*} is inverse to the other characteristic temperatures (T^{**}, T_{MS}, and T_{AS}) of the austenite-martensite phase transition in the $Ni_{49}CuMn_{34}In_{16}$ alloy. Comparing Figs. 6 and 7, it is observed that external pressure and applied magnetic field have opposite effects on the characteristic temperatures T^{**}, T_{MS}, and T_{AS}, as if there is a competition between the two variables. However, the same is not entirely true for the case of T^{*} where the higher values of magnetic field and pressure appear to have similar effects. The elevation of the temperatures T^{**}, T_{MS}, and T_{AS} with increasing pressure might indicate that external pressure supports the martensitic phase. As discussed previously, this could be because of the enhancement of the antiferromagnetic correlations resulting from the shorter Mn–Mn bond lengths in the alloy[4,18–21] because of applied pressure.[24] An enhancement of hybridization of the Ni $3d\ e_g$ states and the $3d$ states of the antiferromagnetically coupled (extra) Mn atoms at the In sites[2,23] is also possible because of applied pressure, especially in the presence of the Cu $3d^{10}$ states. However, in the present set of experiments the pressure is applied hydrostatically, and therefore it acts on the sample equally from all directions. This should reduce Ni–Ni and Ni–Mn bond lengths[34] as well. The sign of the exchange interaction between Ni and Mn is reported to be positive both for the Mn atoms occupying their own sites and for those occupying the In sites (due to off-stoichiometry).[35] Probably the ferromagnetic correlations between some of the Ni and Mn atoms in the $Ni_{49}CuMn_{34}In_{16}$ alloy are also enhanced when external pressure is applied, which adds to the existing competition between the antiferromagnetic and ferromagnetic correlations in the alloy.[4,18–21] It may be recalled here that both T_{CA} and T_{CM} were found to increase with increasing pressure indicating an enhancement of ferromagnetic-exchange interaction both in the austenite and martensite phases. Previously Kanomata *et al.* had analyzed the results on a large number of stoichiometric $Ni_{50}Mn_{25}X_{25}$ alloys, where X stands for Al, Ga, In, Sn, and Sb, and inferred that T_{CA} increases with decreasing Mn–Mn distance.[25] The Mn–Mn exchange interaction in the stoichiometric $Ni_{50}Mn_{25}In_{25}$ alloy has been shown to be positive,[35] where the T_{CA} is found to increase with increasing pressure.[25] Thus the work done by Kanomata *et al.* also provides some support to the argument that it might be possible to enhance the ferromagnetic correlations in certain regions of the $Ni_{49}CuMn_{34}In_{16}$ alloy by the application of hydrostatic pressure. Since the austenite phase has higher moment in the present alloy, the ferromagnetic correlations are expected to stabilize the austenite phase of the alloy.[4,18–21] However, these arguments do not clarify why this pressure-induced enhancement of ferromagnetic correlations does not affect the pressure dependence of T^{**}, T_{MS}, and T_{AS}. On the other hand it has been argued previously in this paper that the strain fields produced in the $Ni_{49}CuMn_{34}In_{16}$ alloy are different when the alloy is cooled under applied external pressure from what they are when the alloy is cooled in ambient pressure. The austenite-to-martensite phase transition essentially involves the motion of structural interfaces, which can be hindered by elastic strain.[36] The changed strain fields in the $Ni_{49}CuMn_{34}In_{16}$ alloy in the presence of external pressure probably enhance this hindrance to the motion of the interfaces. As a result the supercooled austenite phase persists down to lower temperatures. The enhanced ferromagnetic correlations in some crystallographic sites of the alloy might provide some assistance to this hindrance by making the austenite phase more favorable in certain locations. This also seems to be consistent with the observation that the higher values of magnetic field and pressure appear to have similar effects on the T^{*} for the austenite-martensite phase transition in the present alloy.

The pressure gradient of T_{MS} provides a method to calculate (approximately) the volume change expected in the

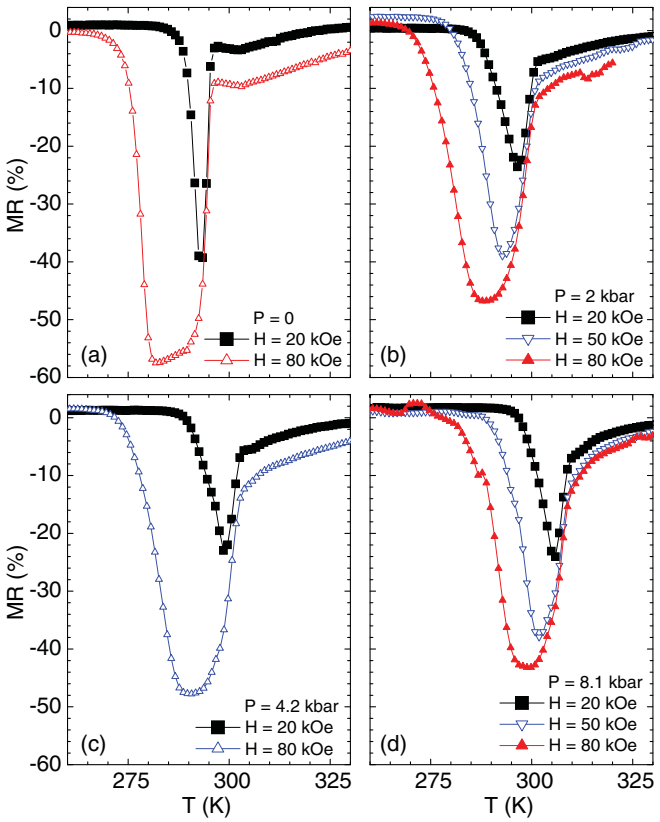

FIG. 8. (Color online) The temperature dependence of MR of the $Ni_{49}CuMn_{34}In_{16}$ alloy for different values of external pressure. The MR is estimated using the electrical resistivity values measured while warming up the ZFC sample.

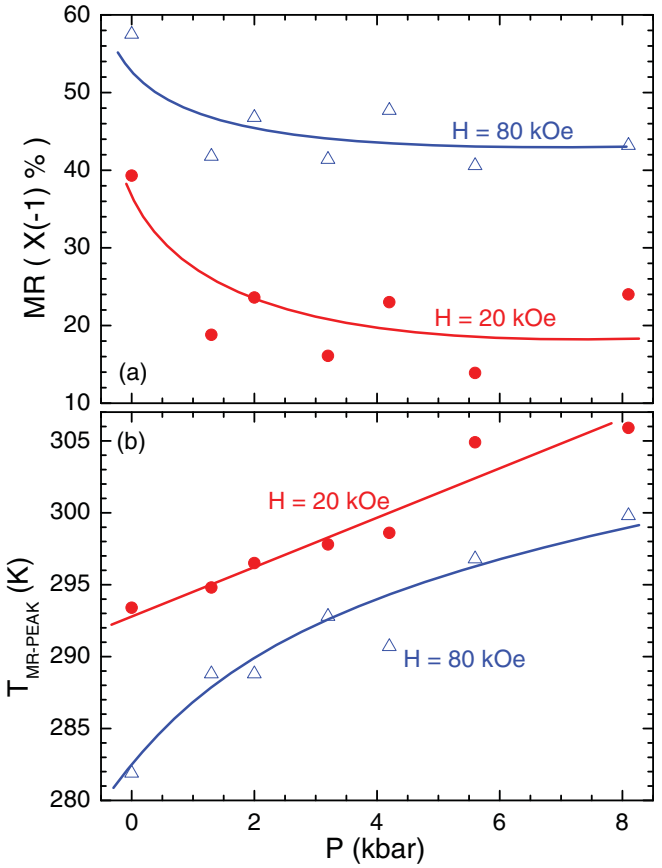

FIG. 9. (Color online) The pressure dependence of (a) the peak magnitude of MR and (b) the temperature at which this peak is observed in 20 and 80 kOe magnetic fields. The solid circles and the open triangles represent the experimental data points for 20 and 80 kOe, respectively. The lines are guides for the eye.

present $Ni_{49}CuMn_{34}In_{16}$ alloy sample across the austenite-to-martensite phase transition. This is done by using the Clausius-Clapeyron equation for a first-order phase transition which may be written as $dT/dP = \Delta V/\Delta S$, where S and V stand for entropy and volume, respectively. The difference of entropy between the austenite and martensite phases in the $Ni_{49}CuMn_{34}In_{16}$ alloy may be taken to be approximately equal to 26 J/kg K.[23] Using $dT/dP = 2$ K/kbar, the value of ΔV is found to be 5.2×10^{-7} m^3/kg. The mass and volume of a unit cell of the $Ni_{49}CuMn_{34}In_{16}$ alloy were obtained using the x-ray diffraction results.[23] Using this information, the relative change of volume ($\Delta V/V$) across the austenite-to-martensite phase transition in the $Ni_{49}CuMn_{34}In_{16}$ alloy was found to be approximately 0.4%. This is of the same order as previously published results for some Ni-Mn-In based off-stoichiometric Heusler alloys.[24] The advantage in the present alloy, however, is that this volume change is obtained near the room temperature.

Since it was noted that the combined effect of external pressure and magnetic field on the different characteristic temperatures of the first-order austenite-martensite phase transition in the $Ni_{49}CuMn_{34}In_{16}$ alloy are quite different from one another, a probe into the role of pressure on the MR observed in this alloy was indeed required for understanding its practical implication. Figure 8 shows the temperature dependence of MR of the $Ni_{49}CuMn_{34}In_{16}$ alloy for different values of external pressure. Here, MR is defined as $MR = \frac{\rho(H)-\rho(0)}{\rho(0)} \times 100$, which denotes the percentage change of resistivity because of applied magnetic field. All the panels of Fig. 8 are plotted in the same scales of T and MR for a clear comparison of MR. Comparing Figs. 4, 5, 6, and 8 it is observed that a large MR is obtained in the $Ni_{49}CuMn_{34}In_{16}$ alloy across the austenite-martensite phase transition. The MR is understood to originate from the field-induced nature of this phase transition and is very small in the temperature regions away from this phase transition. In ambient pressure a peak negative MR of 57.5% is obtained at 281.9 K for an applied magnetic field of 80 kOe. The peak decreases in magnitude but shifts towards higher temperatures with the application of external pressure. Under a pressure of 8.1 kbar, a peak (negative) of 43.2% is observed at 299.8 K. To find how the temperature and magnitude of this peak varies with applied external pressure, these are plotted as a function of pressure and are shown on Fig. 9. It is found [Fig. 9(a)] that the peak magnitude of MR decreases initially with increasing pressure but remains sort of constant (at around 20% for $H =$ 20 kOe and 43% for $H = 80$ kOe) beyond approximately 2 kbar external pressure. On the other hand the temperature at which the peak is observed in the temperature dependence of MR increases approximately linearly with increasing external pressure for $H = 20$ kOe [Fig. 9(b)]. The pressure gradient

of this line is approximately 1.6 K/kbar, which is consistent with that of T_{AS} discussed earlier. The pressure dependence of this peak temperature for $H = 80$ kOe exhibits a weak saturation—like behavior above 2 kbar pressure. The gradient of this line is also close to 1.6 K/kbar beyond 2-kbar pressure. It is observed on Fig. 9(b) that the peak in MR is more effectively elevated to higher temperatures in the presence of 20 kOe magnetic field as compared to 80 kOe magnetic field. For an external pressure of 8.1 kbar this peak is observed at 306 K (approximately) for $H = 20$ kOe, as compared to 300 K (approximately) for $H = 80$ kOe. Figures 9(a) and (b) reveal that a moderate external pressure of 2 kbar and a moderate magnetic field of 20 kOe, in combination, produces approximately 24% (peak) MR in the $Ni_{49}CuMn_{34}In_{16}$ alloy at the ambient temperature of 296.5 K. The effect of applied external pressure can also be generated through chemical pressure that can be achieved by the substitution of atoms in the system. The present results indicate that a chemical pressure induced through a small amount of doping with a nonmagnetic atom, which is equivalent to applying about 2 kbar external pressure, can be quite useful for technological applications. It would now be interesting to see if the functional properties of the $Ni_{50}Mn_{34}In_{16}$ alloys can be enhanced further by slightly increasing the Cu content as compared to the present $Ni_{49}CuMn_{34}In_{16}$ alloy.

IV. SUMMARY AND CONCLUSION

The electrical resistivity of the $Ni_{49}CuMn_{34}In_{16}$ alloy has been studied as a function of temperature, pressure, and magnetic field. It is found that the Curie temperatures in both the austenite and martensite phases increase appreciably with increasing external pressure. It is observed that the resistivity of the alloy in the martensite phase exhibits a large drop in magnitude with the application of 2 kbar pressure. At higher pressures the resistivity attains somewhat higher magnitudes in the martensite phase but does not attain the magnitude obtained in zero pressure. In the austenite phase, however, both the magnitude of resistivity and its temperature gradient decrease with increasing external pressure. It is observed that this anomalous behavior of resistivity in the martensite phase in the presence of pressure is not affected by applied magnetic field and is therefore not related to the magnetic interactions in the alloy. Comparing with the previously published results on large strain produced with varying temperature in the martensite phase of the $Ni_{49}CuMn_{34}In_{16}$ alloy,[23] it is conjectured that external pressure affects the strain and strain-disorder coupling in the $Ni_{49}CuMn_{34}In_{16}$ alloy. This has strong influence on the scattering of conduction electrons in the martensite phase. The magnetic field dependence of the onset temperatures of the austenite-to-martensite (while cooling down) and martensite-to-austenite (while warming up) phase transitions and that of the temperature limit of supercooling of the austensite phase are determined. These field-temperature lines are found to be elevated toward higher temperatures with increasing pressure. This might indicate the enhancement of the hybridization of the Ni 3*d* states and the 3*d* states of the antiferromagnetically coupled (extra) Mn atoms at the In sites[22,23] and/or reduction of the Mn–Mn distance as a result of applied external pressure.[24] However, the field-temperature phase line corresponding to the temperature limit of supercooling of the austensite phase is found to exhibit an opposite trend. It is conjectured that the strain fields produced in the $Ni_{49}CuMn_{34}In_{16}$ alloy are different when the alloy is cooled under applied external pressure from what they are when the alloy is cooled in ambient pressure. These changed strain fields probably enhances the hindrance to the motion of the structural interfaces across the austenite-to-martensite phase transition in the alloy in the presence of external pressure and help the supercooled austenite phase to persist down to lower temperatures. From the pressure dependence of the onset temperature for the austenite-to-martensite phase transition, the volume change expected in the alloy across this phase transition has been estimated using the Clausius-Clapeyron equation. This comes out to be approximately 0.4%, which is substantial and shows the potential of the alloy for near room temperature actuator applications. Moreover, a MR of magnitude as high as 57.5% is obtained in the alloy at 281.9 K for an applied magnetic field of 80 kOe. It is shown that a combination of an external pressure of 2 kbar and a magnetic field of 20 kOe can produce a MR of 24%, approximately, in the $Ni_{49}CuMn_{34}In_{16}$ alloy at the ambient temperature of 296.5 K. This knowledge could be utilized for designing newer alloys through the application of chemical pressure, so as to obtain large MR and other functional properties in this alloy system at room temperature.

ACKNOWLEDGMENT

The authors are thankful to Mr. R. K. Meena for his help in sample preparation.

*maulindu@rrcat.gov.in

[1] Y. Sutou, Y. Imano, N. Koeda, T. Omori, R. Kainuma, K. Ishida, and K. Oikawa, Appl. Phys. Lett. **85**, 4358 (2004).

[2] K. Oikawa, W. Ito, Y. Imano, Y. Sutou, R. Kainuma, K. Ishida, S. Okamoto, O. Kitakami, and T. Kanomata, Appl. Phys. Lett. **88**, 122507 (2006).

[3] T. Krenke, M. Acet, E. F. Wassermann, X. Moya, L. Manosa, and A. Planes, Phys. Rev. B **73**, 174413 (2006).

[4] T. Krenke, E. Duman, M. Acet, E. F. Wassermann, X. Moya, L. Manosa, A. Planes, E. Suard, and B. Ouladdiaf, Phys. Rev. B **75**, 104414 (2007).

[5] V. K. Sharma, M. K. Chattopadhyay, and S. B. Roy, J. Phys. D **40**, 1869 (2007).

[6] A. K. Pathak, M. Khan, I. Dubenko, S. Stadler, and N. Ali, Appl. Phys. Lett. **90**, 262504 (2007).

[7] X. Moya, L. Mañosa, A. Planes, S. Aksoy, M. Acet, E. F. Wassermann, and T. Krenke, Phys. Rev. B **75**, 184412 (2007).

[8] V. K. Sharma, M. K. Chattopadhyay, K. H. B. Shaeb, A. Chouhan, and S. B. Roy, Appl. Phys. Lett. **89**, 222509 (2006).

[9] B. M. Wang, L. Wang, Y. Liu, B. C. Zhao, Y. Zhao, Y. Yang, and H. Zhang, J. Appl. Phys. **106**, 063909 (2009).

[10]B. Zhang, X. X. Zhang, S. Y. Yu, J. L. Chen, Z. X. Cao, and G. H. Wu, Appl. Phys. Lett. **91**, 012510 (2007).
[11]L. S. Sharath Chandra, M. K. Chattopadhyay, V. K. Sharma, S. B. Roy, and S. K. Pandey, Phys. Rev. B **81**, 195105 (2010).
[12]A. Planes, L. Manosa, and M. Acet, J. Phys. Condens. Matter **21**, 233201 (2009).
[13]L. Mañosa, D. Gonzalez-Alonso, A. Planes, E. Bonnot, M. Barrio, J.-L. Tamarit, S. Aksoy, and M. Acet, Nat. Mater. **9**, 478 (2010).
[14]J. Kubler, A. R. Williams, and C. B. Sommers, Phys. Rev. B **28**, 1745 (1983).
[15]E. Sasioglu, L. M. Sandratskii, and P. Bruno, Phys. Rev. B **70**, 24427 (2004).
[16]E. Şaşıoğlu, L. M. Sandratskii, and P. Bruno, Phys. Rev. B **77**, 064417 (2008).
[17]Y. Sutou, Y. Imano, N. Koeda, T. Omori, R. Kainuma, K. Ishida, and K. Oikawa, Appl. Phys. Lett. **85**, 4358 (2004).
[18]P. A. Bhobe, K. R. Priolkar, and P. R. Sarode, J. Phys. D: Appl. Phys. **41**, 045004 (2008).
[19]P. A. Bhobe, K. R. Priolkar, and A. K. Nigam, J. Phys. D: Appl. Phys. **41**, 235006 (2008).
[20]S. Aksoy, M. Acet, P. P. Deen, L. Mañosa, and A. Planes, Phys. Rev. B **79**, 212401 (2009); V. V. Khovaylo, T. Kanomata, T. Tanaka, M. Nakashima, Y. Amako, R. Kainuma, R. Y. Umetsu, H. Morito, and H. Miki, *ibid*. **80**, 144409 (2009).
[21]V. K. Sharma, M. K. Chattopadhyay, and S. B. Roy, J. Phys. Condens. Matter **20**, 425210 (2008).
[22]M. Ye, A. Kimura, Y. Miura, M. Shirai, Y. T. Cui, K. Shimada, H. Namatame, M. Taniguchi, S. Ueda, K. Kobayashi, R. Kainuma, T. Shishido, K. Fukushima, and T. Kanomata, Phys. Rev. Lett. **104**, 176401 (2010).
[23]V. K. Sharma, M. K. Chattopadhyay, A. Khandelwal, and S. B. Roy, Phys. Rev. B **82**, 172411 (2010).
[24]L. Mañosa, X. Moya, A. Planes, O. Gutfleisch, J. Lyubina, M. Barrio, J-L. Tamarit, S. Aksoy, T. Krenke, and M. Acet, Appl. Phys. Lett. **92**, 012515 (2008).
[25]T. Kanomata, K. Shirakawa, and T. Kaneko, J. Magn. Magn. Mater. **65**, 76 (1987).
[26]L. Patrick, Phys. Rev. **93**, 384 (1954).
[27]F. Albertini, J. Kamarád, Z. Arnold, L. Pareti, E. Villa, and L. Righi, J. Magn. Magn. Mater. **316**, 364 (2007); J. Kamara'd, F. Albertini, Z. Arnold, F. Casoli, L. Pareti, A. Paoluzi, *ibid*. **290–291**, 669 (2005); K. Mandal, D. Pal, N. Scheerbaum, J. Lyubina, and O. Gutfleisch, J. Appl. Phys. **105**, 073509 (2009).
[28]Y. Chieda, T. Kanomata, K. Fukushima, K. Matsubayashi, Y. Uwatoko, R. Kainuma, K. Oikawa, K. Ishida, K. Obara, and T. Shishido, J. Alloys Compd. **486**, 51 (2009).
[29]M. K. Chattopadhyay, M. A. Manekar, V. K. Sharma, Parul Arora, P. Tiwari, M. K. Tiwari, and S. B. Roy, J. Appl. Phys. **108**, 073909 (2010).
[30]S. Kartha, J. A. Krumhansl, J. P. Sethna, and L. K. Wickham, Phys. Rev. B **52**, 803 (1995); J. Burgy, A. Moreo, and E. Dagotto, Phys. Rev. Lett. **92**, 097202 (2004); P. A. Sharma, S. B. Kim, T. Y. Koo, S. Guha, and S.-W. Cheong, Phys. Rev. B **71**, 224416 (2005).
[31]P. M. Chaikin and T. C. Lubensky, *Principles of Condensed Matter Physics* (Cambridge University Press, Cambridge, England, 1995).
[32]Y. Imry and M. Wortis, Phys. Rev. B **19**, 3580 (1980).
[33]M. K. Chattopadhyay, S. B. Roy, A. K. Nigam, K. J. S. Sokhey, and P. Chaddah, Phys. Rev. B **68**, 174404 (2003); S. B. Roy, G. K. Perkins, M. K. Chattopadhyay, A. K. Nigam, K. J. S. Sokhey, P. Chaddah, A. D. Caplin, and L. F. Cohen, Phys. Rev. Lett. **92**, 147203 (2004).
[34]W. Ito, Y. Imano, R. Kainuma, Y. Sutou, K. Oikawa, and K. Ishida, Metall. Mater. Trans. A **38A**, 759 (2007); T. Kanomata, T. Yasuda, S. Sasaki, H. Nishihara, R. Kainuma, W. Ito, K. Oikawa, K. Ishida, K.-U. Neumann, and K. R. A. Ziebeck, J. Magn. Magn. Mater. **321**, 773 (2009).
[35]V. D. Buchelnikov, P. Entel, S. V. Taskaev, V. V. Sokolovskiy, A. Hucht, M. Ogura, H. Akai, M. E. Gruner, and S. K. Nayak, Phys. Rev. B **78**, 184427 (2008).
[36]P. A. Sharma, S. El-Khatib, I. Mihut, J. B. Betts, A. Migliori, S. B. Kim, S. Guha, and S.-W. Cheong, Phys. Rev. B **78**, 134205 (2008).